Effect of fiber orientation-based composite lamina on mitigation of stress intensity factor for a repaired plate: a finite element study

Abdul Aabid*, Muneer Baig
Department of Engineering Management, College of Engineering Prince Sultan University, PO BOX 66833, Riyadh 11586, Saudi Arabia
aaabid@psu.edu.sa, mbaig@psu.edu.sa

Meftah Hrairi, Jaffar Syed Mohamed Ali
Department of Mechanical and Aerospace Engineering, Faculty of Engineering, International Islamic University Malaysia, P.O. Box 10, 50725 Kuala Lumpur, Malaysia
meftah@iium.edu.my, jaffar@iium.edu.my

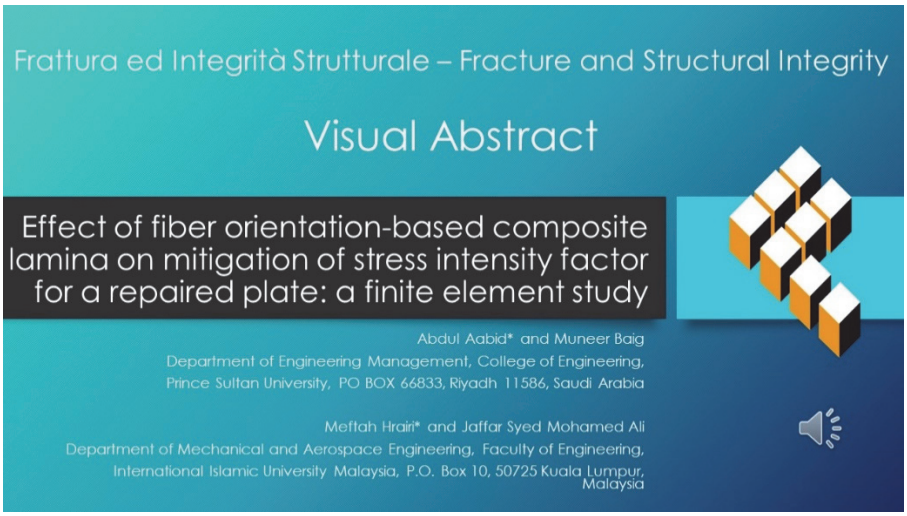

Citation: Aabid, A., Baig, M., Hrairi, M., Mohamed Ali, J. S., Effect of fiber orientation-based composite lamina on mitigation of stress intensity factor for a repaired plate: a finite element study, Frattura ed Integrità Strutturale, 68 (2024) 209-221.

Received: 25.12.2024
Accepted: 30.01.2024
Published: 09.02.2024
Issue: 01.04.2024

KEYWORDS. Composite patch, Stress intensity factor, Fiber direction, FEM, Thin-walled structure.

INTRODUCTION

Fatigued components are commonly repaired while in use, typically through standard repair methods that involve the consolidation of the component by attaching a strengthening element using bolts or rivets. This process helps reduce the stress intensity factors (SIFs) at the crack tip. Over the past two decades, advancements in composite materials and adhesive bonding have introduced more efficient repair techniques. Bonded composite repair technique offer benefits like ensuring minimal stress concentration effects during load transfer between the host structure and bonded patch, allowing customization of the material properties and design of the bonded patch for specific applications, and avoiding significant additional weight to the component with the use of composite repair patches.

In the literature, the bonded composite repair is considered with numerical and experimental investigation in most of the work. Some of the related work has been explored in this literature to differentiate and extract the contribution of this work. Nayak [1] emphasized the efficiency of composite materials for bonded repair, while Guruprasad [2] investigated the influence of composite patches on an aluminium crack plate and demonstrated the reduction in fracture parameter (SIF) through experimental and numerical investigations. Further studies have confirmed the effectiveness of composite patching on SIF reduction, including the use of a side-bonded patch through a p-convergent layered model [3] and the combination of genetic algorithms and the finite element (FE) method to measure SIF under temperature effects [4]. Moreover, nontraditional composite patch ply orientations have been examined for open-hole scarfed panels [5], and the fracture performance of cracked panels repaired with a bonded patch has been predicted for thick/thin metallic panels [6,7] and wood beams [8].

Extensive research has been conducted on employing composite patches to repair cracked plates, with scholars investigating various shapes and modifications to enhance repair effectiveness [9, 10]. Aabid et al. [11] demonstrated the utilization of composite patches with varied parameters in their studies. Makwana and Shaikh [12] examined the hybridization of different fiber volume fractions in composite patches with varying stiffness for minimizing the SIF. The study demonstrated the combination of bonding and drilled holes knowing a hybrid repair approach to repair the aircraft structures (thin-plates) through elastoplastic analysis [13]. After repairing a cracked structure with a composite patch, researchers have also observed mechanical behavior to investigate the effects of resin properties and repair configuration [14]. Studies on composite patch repair have also been conducted on multiple cracks [15], inclined cracks [16], cracks from circular notches [17], and other fracture parameters, such as fatigue performance [18], J-integral evaluation [19], energy release rate [20], concentration factor [21, 22], humidity effect [23], and multiple material combination [24] involving composites. Also, the bonded repair method was used to investigate low-velocity impact damage evaluation [25], and overlay patch repair of scratch damage in laminated composites [26] for the application of aircraft structures.

After conducting the literature on bonded composite repairs for mode-1 crack propagation, it was found that different patch materials were employed to improve repair performance. Additionally, variations in patch dimensions and shapes were observed within the same area. Achieving an effective design for the reinforcement (composite patch) requires estimating the resulting SIF at the crack tip in the patched panel. Despite this research and the authors' extensive knowledge from the past two decades, attention has not been given to the influence of the fiber direction of a given composite patch on the repair of cracked plates for mode-I crack propagation. Thus, the primary contribution of the current work is to identify the effectiveness of fiber direction in enhancing bonded composite repair performance. Therefore, this study was conducted to address this gap and improve the quality of bonded composite repair performance in the current era.

PROBLEM FORMULATION

The use of a rectangular patch shape, while acknowledged as not the optimal choice, serves as a valuable tool for gaining insights into mechanical efficiency and developmental aspects [27]. This shape signifies the minimal patch size necessary to adequately cover the crack length, leading to a nuanced understanding of mechanical behavior during loading conditions [28].

To examine the effect of fiber orientation on the glass/epoxy composite patch in an aluminium alloy 2024-T3 center-cracked rectangular plate, a host specimen was chosen under a uniform uniaxial tensile load of 1 MPa for repair performance [29]. The aluminium alloy possesses properties such as a density of 2715 kg/m^3, Poisson's ratio of 0.33, and Young's modulus of 68.95 GPa, along with dimensions of 200 mm in height, 40 mm in width, and 1 mm in thickness. In contrast, the composite properties, detailed in Tab. 1, include dimensions of 20 mm in height/width and 0.5 mm in thickness. The plate features a 20-mm crack at the center, and a composite patch is fully bonded to the cracked area using Araldite 2014 adhesive. The adhesive bond has properties including a density of 1160 kg/m^3, Poisson's ratio of 0.345, Young's modulus of 5.1 GPa, and shear modulus of 1.2 GPa, with dimensions of 20 mm in height/width and 0.03 mm in thickness. Fig. 1 illustrates the complete model for the analytical and simulation investigation, while for the simulation, only the quarter model was considered to save time and energy.

The primary objective of this investigation is the effect of fiber orientation on repair performance, and Fig. 2 shows the actual direction of the fiber that is considered in the present work. A total of three directions have been considered; the names can be seen in the caption of Fig. 2. The mechanical properties generally show high strength in the direction of the fiber. The current work employed the glass/epoxy composite as a bonded composite material due to its excellent characteristic load transfer [30–33]. Furthermore, to change the direction of fiber, a simple assumption was made by changing the properties with numeric values as per the fiber directions.

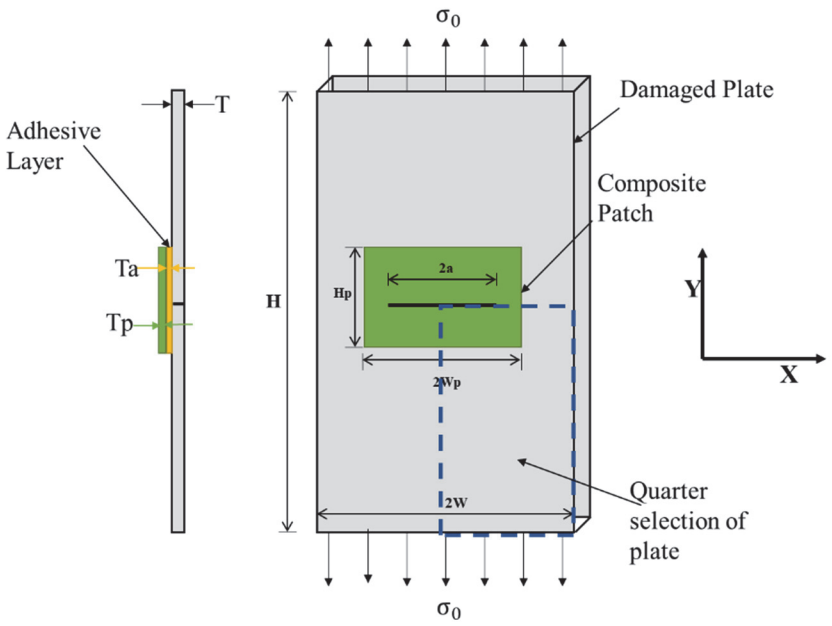

Figure 1: Problem formulation of a center-cracked plate.

Parameter	Type 1	Type 2	Type 3
Poisson's Ratio υ12	0.30	0.35	0.35
Poisson's Ratio υ13	0.35	0.30	0.35
Poisson's Ratio υ23	0.35	0.35	0.30
Young's Modulus (E1)	16.68 GPa	03.69 GPa	16.68 GPa
Young's Modulus (E2)	03.69 GPa	16.68 GPa	16.68 GPa
Young's Modulus (E3)	03.69 GPa	03.69 GPa	03.69 GPa
Shear Modulus (G12)	02.56 GPa	02.24 GPa	02.56 GPa
Shear Modulus (G13)	02.24 GPa	02.56 GPa	02.56 GPa
Shear Modulus (G23)	02.24 GPa	02.24 GPa	02.24 GPa
Isotropic view of the lamina composite plate	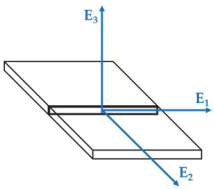	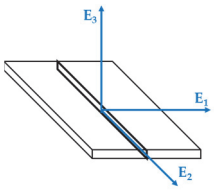	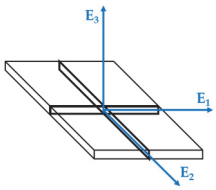

Table 1. Materials properties of the glass/epoxy.

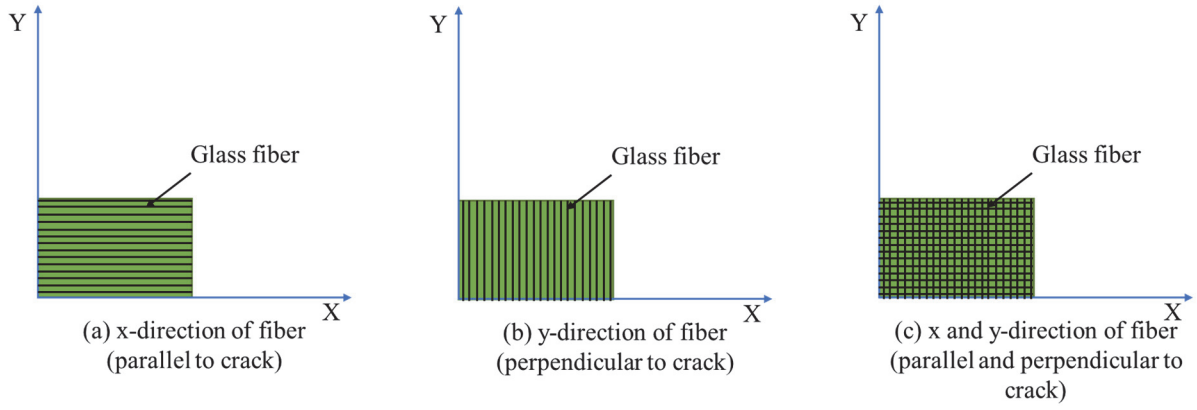

Figure 2: Composite patch fiber directions.

FINITE ELEMENT (FE) METHOD

The ANSYS commercial software with APDL was used with the coding method. The present work simplified the fracture mechanics parameters through the FE method. In fracture mechanics, the study of failure structures concerning their material can play a key role in the elastic region and therefore this work is limited to LEFM because the thin plate was used.

Crack Tip Modeling

In crack tip displacement analysis (Fig. 3), there is a high-stress gradient needed in the region around the crack tip to measure SIF and because of this, the FE modeling required more attention in this specific region. This can be solved by both two-dimensional and three-dimensional modeling and the terminology used for the crack tip with representation around the crack region is slightly different. To define the crack tip for a 3D model, it should be considered as a crack front.

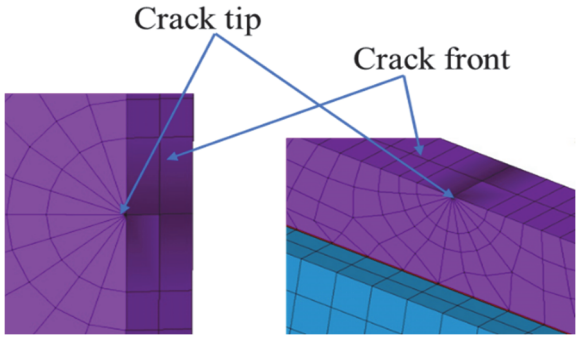

Figure 3: Illustration of the crack tip and crack front for the present FE model

Singular elements suggested by Barsoum, [34] which is utilized to find a reasonable sign of the crack tip displacement. For LEFM problems, near the crack front, the displacement varies as $\sqrt{r}$, where r is the distance from the crack tip. At the crack end, the stress and pressure are special, changing as $\frac{1}{\sqrt{r}}$. Using the KCALC command, the stress intensity at the crack for a linear elastic analysis is computed. The study fits nodal displacement near the crack and location procedure [35],

$$K_I = \sqrt{2\pi}\frac{2G}{1+k}\frac{|V|}{\sqrt{r}} \tag{1}$$

For the others, where $|V|$ is the face split motion. The final term of the Eqn. (1) factor $\frac{|V|}{\sqrt{r}}$, which must be assessed and proven on nodal displacement and locations. V normalizes so that V is 0 at node I (r = 0). Then A and B determined so that,

$$\frac{|V|}{\sqrt{r}} = A + Br \tag{2}$$

at point J and K. Next, let r approaches 0, then it becomes,

$$\lim_{r\to 0}\frac{|V|}{\sqrt{r}} = A \tag{3}$$

thus Eqn. (1) becomes,

$$K_I = \sqrt{2\pi}\frac{2GA}{1+k} \tag{4}$$

Then Eqn. (4) gives nodal displacement to the SIF, based on the singular variable. The displacement near the tip of the crack is obtained from the analysis of finite elements. Fig. 4 shows the singular element around the crack tip with the present numerical work.

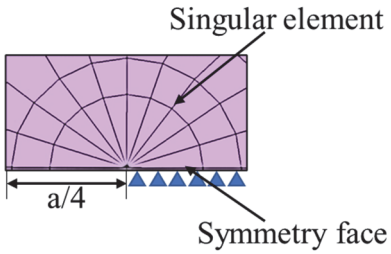

Figure 4: Illustration of the singular element from the present FE model.

Crack plate modeling

Fig. 5 shows the rectangular plate model without and with mesh. The plate has been modeled with fields of stress and deformation around the tip of the crack with a high-stress gradient. The crack tip mesh should have certain characteristics: The crack face should match to create consistency in stresses and strains.

The present model was built with the SOLID186 element which is available in the ANSYS APDL directory. Generally, this type of element contains twenty-nodded elements with a higher-order degree of freedom. For mesh, it employed a total of 10 singular elements to model the crack front for the quarter model. To create a singular element in a plate the crack tip key point was picked and selected as the concentration point to split the element division with a radius of first-row elements around the circumfix'. Next, skewed one by the fourth point for changing the node to a mid-side position, and the lines split into several element divisions with a spacing ratio of 0.2. which is connected to the crack tip and other lines are split into a number of element divisions. After assigning the elements for the mesh a total of 18,890 high-ordered reduced integrated solid elements were formed and it is used for the host plate mesh model.

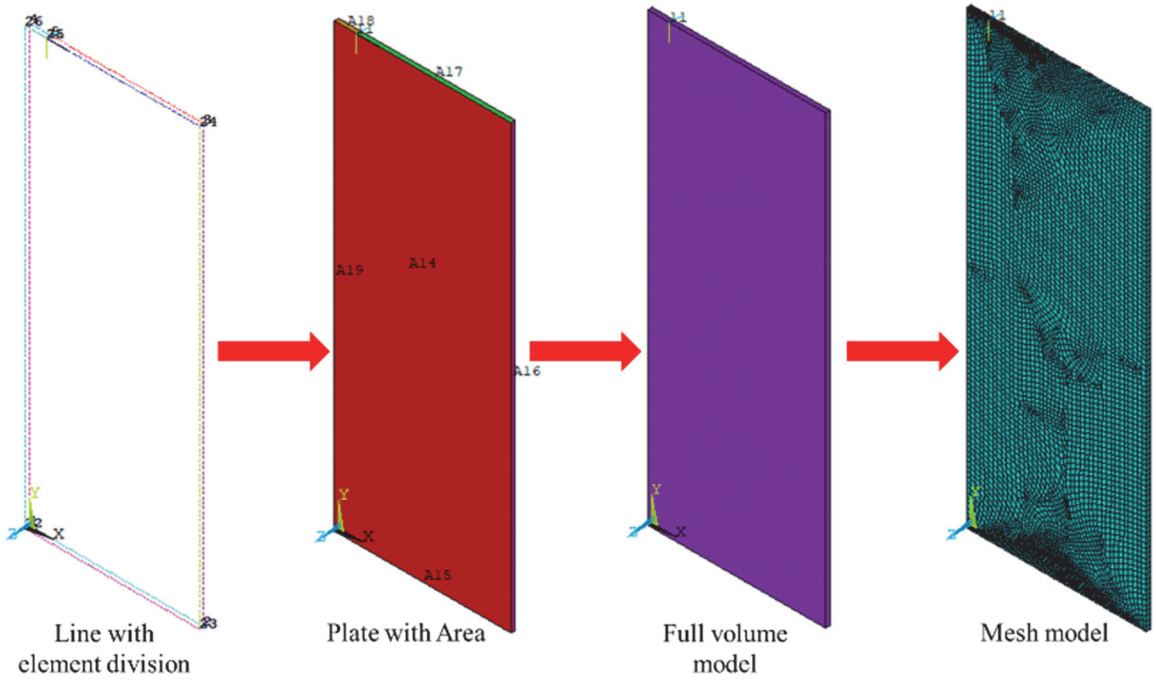

Figure 5: Modelling of plate

Adhesive bond and composite patch modeling

The property of the composite patch is used to define the patch in the FE method for passive repair. In this case, the composite patch is considered glass/epoxy, and the type of element SOLID186 is used to model the patch and adhesive bond. Just a quarter of the full model was designed due to symmetry to save run time. The adopted FE mesh consisted of

3,199 coupling-field elements that were used to model the patch by considering the element size to be 0.0004 m. Similarly, with the same mesh size, an adhesive model was built, and 1,900 reduced integrations of solid elements for an adhesive bond were used.

Complete FE model and boundary conditions

The complete set of FE models considering all aspects of the quarter model can be seen in Fig. 6(a), which is built based on the defined boundary conditions as indicated in Fig. 6(b). The uniform uniaxial load of 1 MPa is applied perpendicular to the crack length on both sides of the full plate or one side of the present quarter model. Whereas to make symmetry, the model is fixed at quarter lines with displacing at the x- and y-direction, considering 0 or fixed. In the case of the adhesive bond and composite patch, a similar term has been implemented to make them fixed on quarter lines. In addition, the z-direction of the plate is fixed (no moment is assumed), and the displacement only occurs in the y-direction when the static load is applied to the plate.

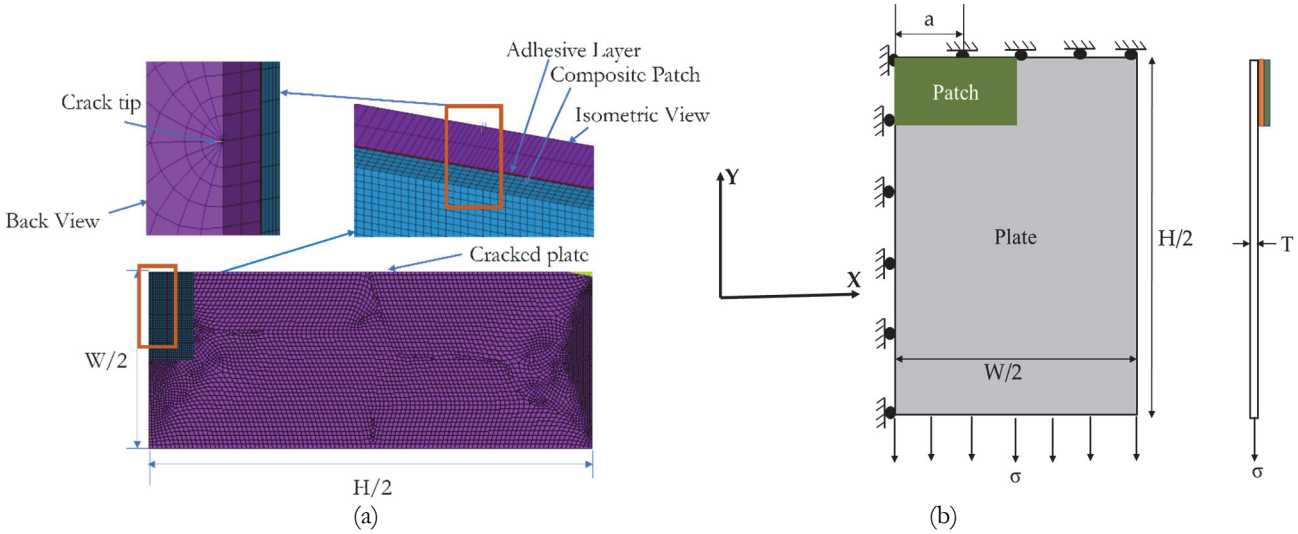

Figure 6: Complete set of the model (a) FE model (b) boundary conditions

RESULTS AND DISCUSSION

In the results section, a deep analysis of bonded composite repair is shown, considering all possible parameters with fiber orientation effects. For the first, the FE method was validated with benchmark results, and a grid independence test was performed for optimal mesh determination. Then, plate crack length and composite parameters varied depending on the effect of SIF. Later, the authors compared all methodologies adopted in this study with a parametric investigation for the determination of optimal results for SIF.

Validation of the FE method

The repaired model was evaluated and compared with existing experimental findings referenced in the study [21]. To ascertain the fidelity of the FE model, it was essential to replicate established benchmark outcomes using a comparable model and parametric sets. The test item, fabricated by Lexas, was a printed circuit board assembly featuring an edge crack. This was accompanied by a bonded Plexiglas patch subjected to uniform tensile stress. The dimensions of the cracked plate were meticulously measured: 100 mm in width, 200 mm in length, and 2 mm in thickness, with a crack extending 40 mm. The Plexiglas patch matched the width of the plate at 100 mm, while its length and thickness varied between 80 and 200 mm and 2 and 4 mm, respectively. This study emphasized the FE model, yielding results that closely aligned with existing experimental data. The foundation of these findings rested on accurate modelling, with particular emphasis on boundary conditions as a pivotal aspect of the analysis. As illustrated in Fig. 7 of the current study, the FE model exhibited exceptional performance. The deviation from Papadopoulos et al. experimental outcomes [21] was minimal, with a relative error under 10%, underscoring the precision and reliability of the current modelling approach.

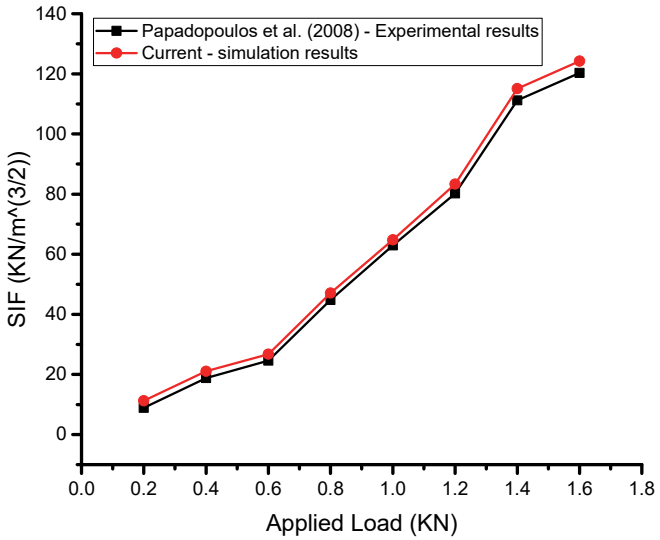

Figure 7: Validation of current simulation results with existing experimental study

Grid independence test

In the crack plate-FE model, special attention is needed to the crack region, particularly at the crack tip due to the high-stress gradient that occurs. For accuracy in simulation results, around the crack tip, the first row of elements must have an a/8 radius or less than this (a = crack length), and the angle between each element varies from 15 to 30 degrees along the circular crack front. Also, the crack tip elements are not one-sided, and the shape must be in isosceles triangles (ANSYS help 18.0). The effect of mesh changes around the crack tip on NSIF can be seen in Fig. 8.

The grid independence test is important to understand mesh criteria for a specific problem. The case chosen for the grid independence test is a center-crack plate with a composite patch of fiber direction 1 and a crack length of 10 mm. The singular element size around the crack tip varied from 1 to 18 percent of the total crack length for the mesh study. The obtained results show the consistency is limited to nine percent or less, this limit is within the ANSYS recommendation range. In addition, when element size is varied the ratio between each row is set to 0.2 for accuracy purposes; indeed, this is also recommended by previous scholars [36]. Furthermore, the simulation of this article has performed in a range of 5% of the total crack length in all cases, which is consistent with the obtained results.

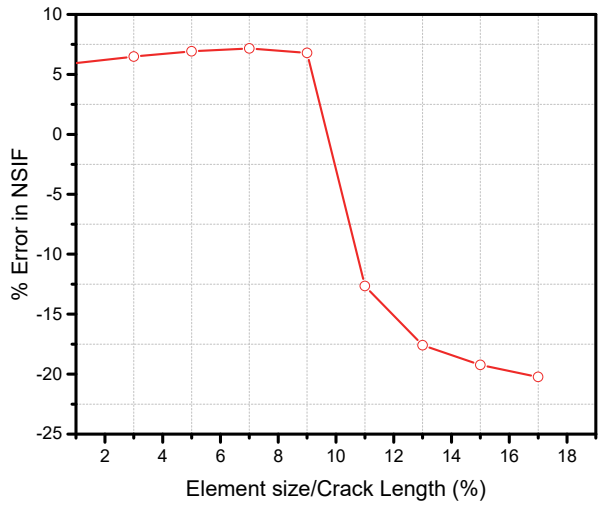

Figure 8: Convergence study % error of NSIF of a center-cracked repaired plate

Parametric Studies through FE Modeling

A numerical approach is considered a major result of this study because all parameters can be determined. The results obtained for all three types of fiber directions for lamina composite repair are the primary objective of this work. Then, a

closed-form analytical model and different ML algorithms were explored, and the SIFs were obtained with the comparison of the present numerical results as a secondary objective of the current work.

Effect of crack length

The crack length's impact has been examined for all three types of fiber orientations of the bonded patch on the crack area. This analysis aims to compare the reinforcement effect among them. The results presented in Fig. 9 were obtained using the FE method. The primary objective of these findings is to assess the strength of the bonded patch on the cracked plate by measuring the reduction in SIF. In this study, a glass/epoxy composite patch was utilized, and its properties were adjusted according to the orientation of the fiberglass. It is widely acknowledged that fiber direction typically imparts greater strength compared to the matrix material. However, the literature lacks sufficient investigations concerning the bonded composite patch repair of a cracked plate, considering different fiber orientations. Consequently, this research provides valuable insights into the effects of crack length using three distinct fiber directions for glass/epoxy composite patches. As stated in the problem formulation, the first type of glass/epoxy patch is oriented parallel to the crack length, meaning that the fibers are stronger along the x-axis. However, since the load is applied along the y-axis, the SIF is lower compared to the other two types. For example, in the type I case, the maximum reduction in SIF was observed for a crack length of 15 mm, which amounted to approximately 50%.

On the other hand, when the fiber direction was aligned parallel to the load direction (type II), the results were highly favorable. The SIF reduction reached approximately 77% due to the load-carrying capacity of the fiber direction and the increased effectiveness of shear stress. Notably, when examining the results for the third type of glass/epoxy patch, they were found to be quite intriguing. The patch exhibited less effectiveness in reducing SIF compared to the second type. In the third type, the fibers were oriented in both the x and y directions, which slightly affected the reinforcement effect in the y direction when the fibers were predominantly oriented in the x direction. As a result, the load effects were distributed differently. Consequently, the maximum SIF reduction observed for the third type of patch was 70%. The present work demonstrates that the fiber direction of the composite patch significantly influences its reinforcement effectiveness. Indeed, similar studies have indicated that the reinforcement effect is more pronounced when the crack is longer, and a composite patch is bonded to the cracked area.

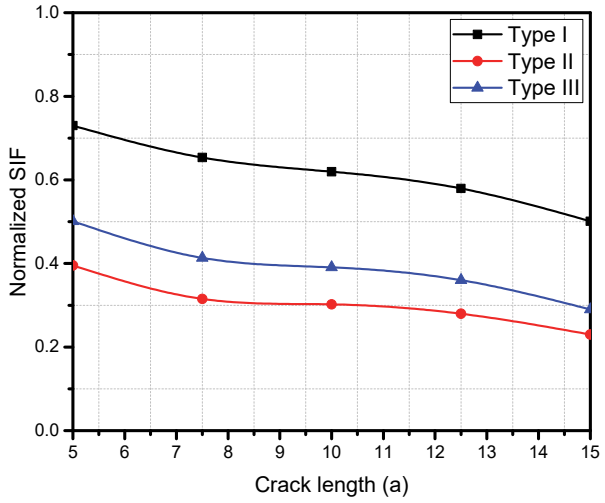

Figure 9: Effect of crack length.

Effect of area ratio

To examine the influence of area ratio on crack repair performance, three different combinations of plates and patches were selected, maintaining the same area ratio while varying their sizes or dimensions. Fig. 10 presents the results of normalized SIF as a function of the area ratio. It is worth noting that the plate and patch thicknesses were consistent across all three sizes, with the plate thickness set at 1 mm and the patch thickness at 0.5 mm. This assumption allowed for a plane stress condition, as discussed in previous sections. Based on the findings from the investigation into the effect of crack length, it was observed that the type II patch was the most effective in reducing SIF. This remained consistent throughout all the parametric studies conducted in this work, with a default crack length of 10 mm chosen for all cases.

When the plate/patch size was small, the stress applied to the perpendicular area was lower, resulting in a higher reduction of SIF due to the smaller reinforced coverage. Conversely, when the plate width increased while applying the same load, there were slight reductions in SIF and a risk of creating a debonded area. This trend continued as the cross-sectional area of the plate patch increased. This study demonstrates that the composite reinforcement significantly affects the change in the normalized SIF fracture parameter, regardless of whether the plate is small or large. Similar studies conducted by Bouiadjra et al. [37] also illustrated that the dimensions of the bonded composite patch, when applied to the same plate, do not have a substantial effect on the variation of normalized SIF at the repaired crack tip, as further confirmed in the subsequent section. However, the current investigation reveals that variations in both plate and patch sizes have a significant impact on the SIF.

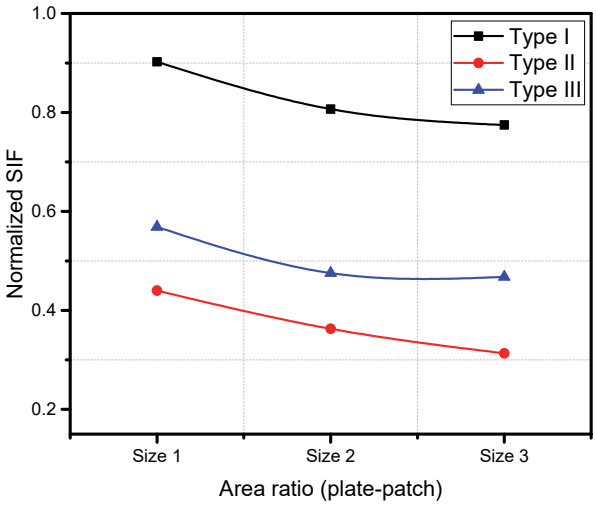

Figure 10: Effect of area ratio

Effect of composite patch size

The effect of composite size will be demonstrated through three types, as illustrated in Fig. 11. It is crucial to characterize the patch size on a bonded plate to investigate the optimal reduction in SIF. Fig. 11(a) presents the effect of patch thickness on normalized SIFs for a crack length of 10 mm. The results indicate that as the patch thickness increases, the normalized SIF decreases. This implies that a thicker patch transfers higher shear stress to the crack area in a relative manner. Notably, when the patch thickness intensifies to approximately 50%, the reductions in normalized SIF follow a similar order. Comparing the results with the patch type, it can be observed that type I shows a slight variation in normalized SIF with changing thickness. Specifically, when the thickness increases from 0.75 mm to 1 mm, the reduction in normalized SIF is slightly less pronounced. However, when the thickness increases from 0.5 mm to 0.75 mm, a proportional reduction in normalized SIF is observed. On the other hand, the other two types exhibit reductions in a similar manner, with type II showing the highest reduction in normalized SIF. Based on these results and analysis, it can be confirmed that selecting a higher patch thickness yields better performance. For achieving suitable stress distribution, it is recommended [38] to utilize multi-layered composite patches for crack repairs.

The width of the composite patch is another critical factor affecting the reduction of SIF. To examine this effect, three different patch widths were chosen for each patch type, and the normalized SIFs were obtained through ANSYS simulations for crack repair. Fig. 11(b) depicts the relationship between patch width and normalized SIFs for a crack length of 10 mm. The reduction in normalized SIF for the center-cracked thin rectangular plate is directly proportional to the patch area's geometry. This effect arises from the increase in patch width, which induces higher stress, resulting in enhanced load transfer through the composite patch. The highest reduction in normalized SIF was observed when the patch width (wp) was set to 20 mm, which falls within the medium range for all three types of composite patches. This finding suggests that a patch width range twice that of the crack length (wp) generates proportional strains in the crack region and facilitates appropriate stress redistribution. Conversely, significant changes in width can lead to imperfect bonding and the formation of a small cohesion zone. This imperfect bonding results in the loss of stress redistribution, as depicted in Fig. 10(b).

Finally, the influence of patch height on the reduction of SIF was investigated, as it also affects the SIF reduction. Similar to thickness and width, three different heights were chosen to examine this effect, and the normalized SIFs were obtained. Fig. 11(c) illustrates the relationship between patch height and normalized SIFs for a crack length of 10 mm. The reduction

in normalized SIF for the plate shows a slight dependence on the height of the patch area. This effect can be attributed to the incremental increase in patch height, which slightly raises induced stress and facilitates greater load transfer through the composite patch. The highest reduction in normalized SIF was observed when the patch height (hp) was set to 25 mm. This range falls within the medium range for all three types of composite patches. This behavior is consistent with the findings discussed earlier regarding patch width, as the same reasoning applies.

In summary, the investigation reveals that the height of the patch also plays a role in the reduction of SIF. Increasing the patch height leads to a slight increase in induced stress, resulting in improved load transfer and a higher reduction in normalized SIF. The optimum reduction was achieved with a patch height of 25 mm, which falls within the medium range for all three types of composite patches.

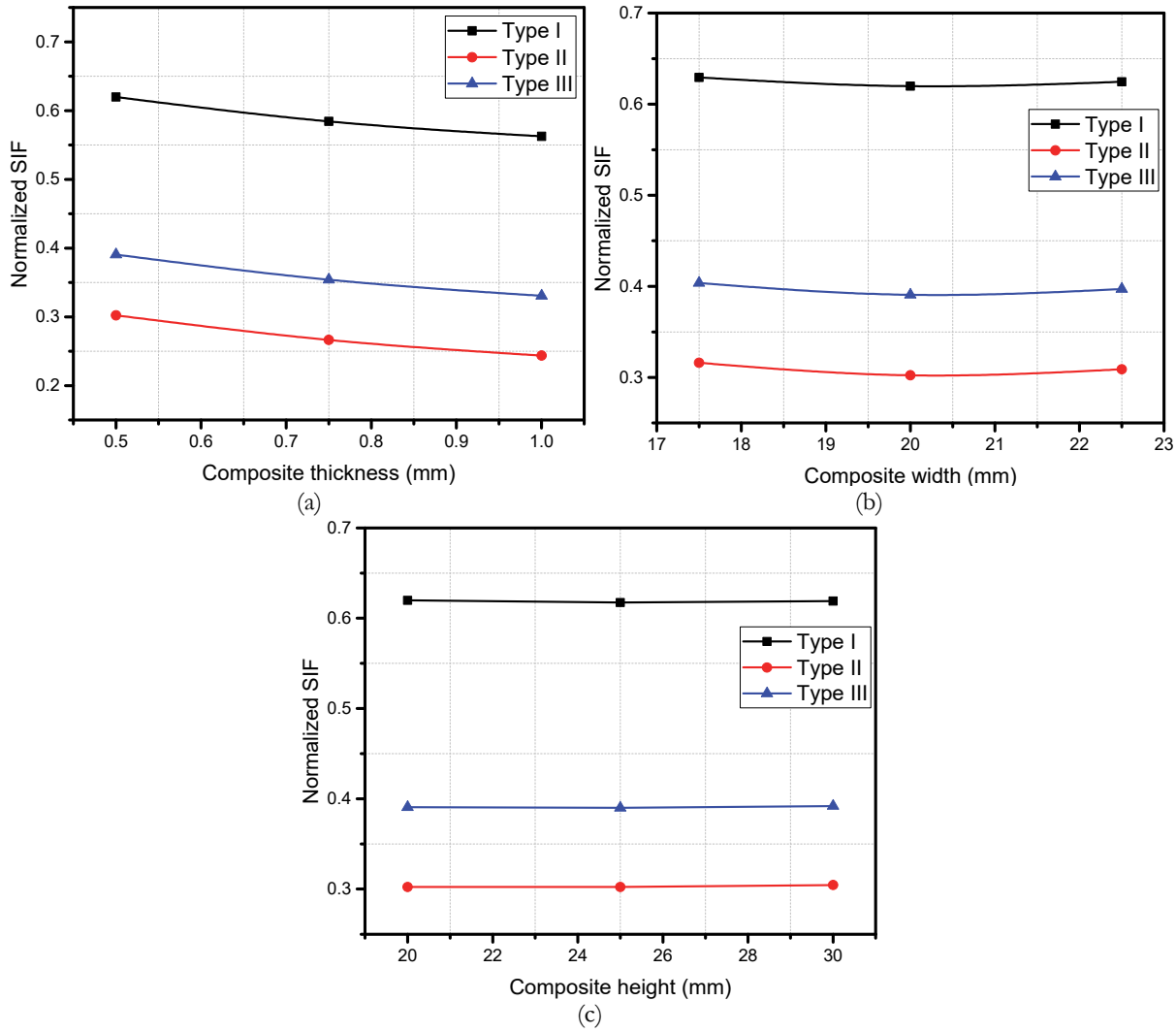

Figure 11: Effect of composite patch size.

Effect of the adhesive bond: Adhesive shear modulus

It is widely recognized that high-quality adhesives possess a low shear modulus, which facilitates the attenuation of stresses transmitted to the adhesive. When it comes to repairing cracks, the objective is to transfer as much stress as possible to the adhesive and, consequently, to the patch to minimize stress at the crack edge. Theoretically, it is preferable to employ adhesives with a high shear modulus (adhesives of lower quality) for patching cracks or defects. Therefore, this section highlights the advantages of adhesive bonding regarding several parameters. Fig. 12 illustrates the relationship between normalized SIF and adhesive shear modulus for crack repair performance.

As per usual, three types of fiber orientation were considered, with a default crack length of 10 mm. Three different variations of the adhesive layer shear modulus were examined to validate the earlier assertions. In fact, the normalized SIF generally decreases as the shear modulus of the adhesive increases. However, the decrease in NSIF tends to diminish as the

shear modulus increases indefinitely in terms of GPa. It is important to note that when the shear modulus of the adhesive bond increases, it may lead to a decrease in the strength of the adhesive, potentially resulting in adhesive failure. Therefore, when selecting an adhesive for crack repair, it is crucial to consider its suitability based on its shear modulus. This ensures effective stress transfer to the patch while preventing adhesive failure caused by excessive stresses in the adhesive layer.

Effect of the adhesive bond: Adhesive thickness

Fig. 13 depicts the relationship between NSIF and adhesive thickness for a crack length of 10 mm. An increase in adhesive thickness had a slight effect on the NSIF, with type I composite patches exhibiting a decrease in NSIF, while the other two types showed a slight increment that remained relatively constant. In existing work [24, 41], it is generally stated that reducing adhesive thickness leads to a decrease in NSIF, indicating that a lower adhesive thickness is preferable for crack repair performance. However, like the findings regarding the influence of adhesive shear modulus, optimizing adhesive thickness is also essential. A thicker patch enhances adhesion but reduces load transfer to the patch, thereby diminishing the advantages of the patch. Conversely, a lower thickness facilitates load transfer to the patch but increases the likelihood of adhesive failure. In summary, while a decrease in adhesive thickness tends to decrease NSIF and is beneficial for crack repair, it is crucial to strike a balance and optimize the adhesive thickness to ensure effective load transfer while minimizing the risk of adhesive failure.

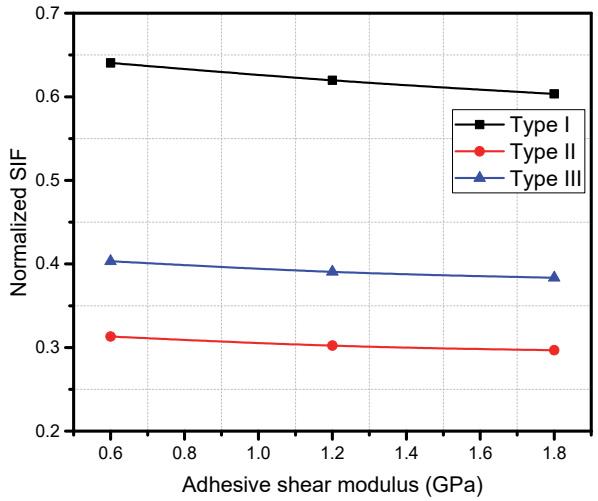

Figure 12: Effect of adhesive shear modulus

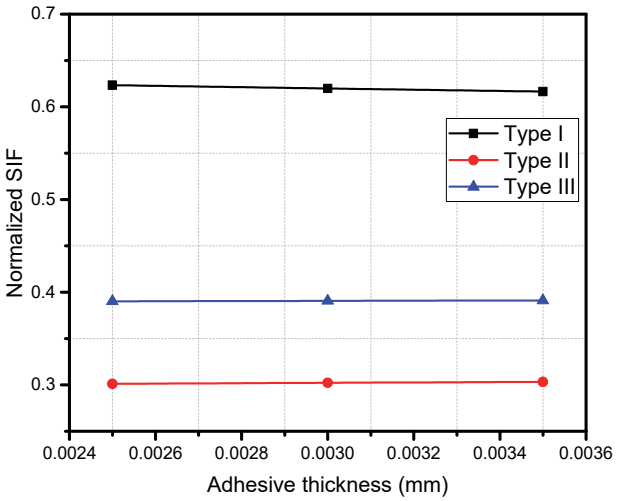

Figure 13: Effect of adhesive thickness.

Conclusion

This study investigated the fracture parameter-SIF in center-cracked aluminium plates that were bonded with different fiber orientation lamina composite patches. The results revealed that crack length, fiber orientation, composite patch parameters, and adhesive bond parameters had a direct influence on the normalized SIF values. The type II fiber direction of glass/epoxy composites exhibited the highest reduction in normalized SIF, while the type I fiber direction showed the lowest reduction. Additionally, as the crack length increased, the normalized SIF values decreased. Furthermore, an increase in the thickness of the bonded composite led to a significant reduction in the normalized SIF values. The study demonstrated the effectiveness of the FE method in determining SIF for both reinforced and non-reinforced plates with composite patches. Overall, this study explored the influence of different parameters on normalizing the SIF values in center-cracked aluminium plates bonded with fiber orientation lamina composite patches. Also, the current investigation highlighted the potential of the fiber direction of composites for repair performance.

Acknowledgement

This research was supported by the Ministry of Education of Malaysia (MOE) through the Fundamental Research Grant Scheme (FRGS/1/2021/TK0/UIAM/01/5). Also, the authors acknowledge the support of the Structures and Materials (S&M) Research Lab of Prince Sultan University

CONFLICTS OF INTEREST

The authors declare no conflict of interest.

AVAILABILITY OF DATA AND MATERIALS

The datasets used during the current study are available from the corresponding author upon reasonable request.

REFERENCES

[1] Nayak, N. V. (2014). Composite materials in aerospace design, Mater. Des., 4(9), pp. 1–10, DOI: 10.1016/0261-3069(96)83772-1.

[2] Guruprasad, K. (1987). Numerical estimation of stress intensity factor, Eng. Fract. Mech., 27(5), pp. 559–69.

[3] Ahn, J.S., Basu, P.K., Woo, K.S. (2010). Analysis of cracked aluminum plates with one-sided patch repair using p - convergent layered model, Finite Elem. Anal. Des., 46(5), pp. 438–48, DOI: 10.1016/j.finel.2010.01.008.

[4] Ergun, E., Tasgetiren, S., Topcu, M. (2012). Stress intensity factor estimation of repaired aluminum plate with bonded composite patch by combined genetic algorithms and FEM under temperature effects, Indian J. Eng. Mater. Sci., 19(1), pp. 17–23.

[5] Breitzman, T.D., Iarve, E. V., Cook, B.M., Schoeppner, G.A., Lipton, R.P. (2009). Optimization of a composite scarf repair patch under tensile loading, Compos. Part A Appl. Sci. Manuf., 40(12), pp. 1921–1930, DOI: 10.1016/j.compositesa.2009.04.033.

[6] Mall, S., Conley, D.S. (2009). Modeling and validation of composite patch repair to cracked thick and thin metallic panels, Compos. Part A Appl. Sci. Manuf., 40(9), pp. 1331–1339, DOI: 10.1016/j.compositesa.2008.08.007.

[7] Duong, C.N. (2009). Design and validation of composite patch repairs to cracked metallic structures, Compos. Part A Appl. Sci. Manuf., 40(9), pp. 1320–1230, DOI: 10.1016/j.compositesa.2008.09.020.

[8] Campilho, R.D.S.G., de Moura, M.F.S.F., Barreto, A.M.J.P., Morais, J.J.L., Domingues, J.J.M.S. (2009). Fracture behaviour of damaged wood beams repaired with an adhesively-bonded composite patch, Compos. Part A Appl. Sci. Manuf., 40(6–7), pp. 852–859, DOI: 10.1016/j.compositesa.2009.04.007.

[9] Baghdadi, M., Serier, B., Salem, M., Zaoui, B., Kaddouri, K. (2019). Modeling of a cracked and repaired Al 2024T3 aircraft plate: Effect of the composite patch shape on the repair performance, Frat. Ed Integrita Strutt., 13(50), pp. 68–85, DOI: 10.3221/IGF-ESIS.50.08.

[10] Li, C., Zhao, Q., Yuan, J., Hou, Y., Tie, Y. (2019). Simulation and experiment on the effect of patch shape on adhesive repair of composite structures, J. Compos. Mater., (100), DOI: 10.1177/0021998319853033.

[11] AAbid, A., Hrairi, M., Ali, J.S.M., Abuzaid, A. (2019). Effect of Bonded Composite Patch on the Stress Intensity Factor For a Center-Cracked Plate, IIUM Eng. J., , DOI: 10.31436/iiumej.v20i2.912.

[12] Makwana, A.H., Shaikh, A.A. (2020). Performance assessment and optimization of hybrid composite patch repair of aircraft structure, Multidiscip. Model. Mater. Struct., 16(5), pp. 887–913, DOI: 10.1108/MMMS-03-2019-0052.

[13] Bouzitouna, W.N., Oudad, W., Belhamiani, M., Belhadri, D.E., Zouambi, L. (2020). Elastoplastic analysis of cracked aluminum plates with a hybrid repair technique using the bonded composite patch and drilling hole in opening mode I, Frat. Ed Integrita Strutt., 14(52), pp. 256–268, DOI: 10.3221/IGF-ESIS.52.20.

[14] Dai, J., Zhao, P., Su, H., Wang, Y. (2020). Mechanical behavior of single patch composite repaired al alloy plates: Experimental and numerical analysis, Materials (Basel)., 13(12), pp. 1–12, DOI: 10.3390/ma13122740.

[15] Srilakshmi, R., Rao, M.V., Kumar, R.S. (2020). Finite element analysis of bonded patch repair of a panel with multiple cracks, AIP Conf. Proc., 2204, DOI: 10.1063/1.5141595.

[16] El-Sagheer, I., Taimour, M., Mobtasem, M., Abd-Elhady, A.A., Sallam, H.E.D.M. (2020). Finite element analysis of the behavior of bonded composite patches repair in aircraft structures, Frat. Ed Integrita Strutt., 14(54), pp. 128–35,

DOI: 10.3221/IGF-ESIS.54.09.
[17] Aabid, A., Hrairi, M., Ali, J.S.M., Abuzaid, A. (2018). Numerical Analysis of Cracks Emanating From Hole in Plate Repaired by Composite Patch, Int. J. Mech. Prod. Eng. Res. Dev., 4(8), pp. 238–243.
[18] Aakkula, J., Saarela, O. (2014). An experimental study on the fatigue performance of CFRP and BFRP repaired aluminium plates, Compos. Struct., 118(1), pp. 589–599, DOI: 10.1016/j.compstruct.2014.07.050.
[19] Belhamiani, M., Belhadri, D.E., Oudad, W., Mansouri, O., Bouzitouna, W.N. (2019). J integral computation and limit load analysis of bonded composite repair in cracked pipes under pressure, Frat. Ed Integrita Strutt., 13(50), pp. 623–637, DOI: 10.3221/IGF-ESIS.50.53.
[20] Kwon, Y.W., Hall, B.L. (2015). Analyses of cracks in thick stiffened plates repaired with single-sided composite patch, Compos. Struct., 119, pp. 727–737, DOI: 10.1016/j.compstruct.2014.09.052.
[21] Papadopoulos, G.A., Badalouka, B., Souyiannis, J. (2008). Experimental study of the reduction at crack-tip stress intensity factor K_I by bonded patch, Int. J. Fract., 149(2), pp. 199–205, DOI: 10.1007/s10704-008-9240-4.
[22] Aabid, A., Hrairi, M., Ali, J.S.M., Abuzaid, A. (2018). Stress Concentration Analysis of a Composite Patch on a Hole in an Isotropic Plate, Int. J. Mech. Prod. Eng. Res. Dev., 6, pp. 249–55.
[23] Sato, M., Yokobori, A.T., Ozawa, Y., Kamiyama, T., Miyanaga, T., Beaumont, P.W.R., Sekine, H. (2002). Experimental study of repair efficiency for single-sided composite patches bonded to aircraft structural panels, Adv. Compos. Mater., 11(1), pp. 51–59, DOI: 10.1163/156855102753613282.
[24] Aabid, A., Hrairi, M., Abuzaid, A., Syed, J., Ali, M. (2021). Estimation of stress intensity factor reduction for a center-cracked plate integrated with piezoelectric actuator and composite patch, Thin-Walled Struct., 158, pp. 107030, DOI: 10.1016/j.tws.2020.107030.
[25] Park, H., Kong, C. (2011). A study on low velocity impact damage evaluation and repair technique of small aircraft composite structure, Compos. Part A Appl. Sci. Manuf., 42(9), pp. 1179–1188, DOI: 10.1016/j.compositesa.2011.05.002.
[26] Shams, S.S., El-Hajjar, R.F. (2013). Overlay patch repair of scratch damage in carbon fiber/epoxy laminated composites, Compos. Part A Appl. Sci. Manuf., 49, pp. 148–156, DOI: 10.1016/j.compositesa.2013.03.005.
[27] Mahadesh Kumar, A., Hakeem, S.A. (2000). Optimum design of symmetric composite patch repair to centre cracked metallic sheet, Compos. Struct., 49(3), pp. 285–292, DOI: 10.1016/S0263-8223(00)00005-2.
[28] Ricci, F., Franco, F., Monrefusco, N. (2011).Bonded Composite Patch Repairs on Cracked Aluminum Plates: Theory, Modeling and Experiments. Advances in Composite Materials - Ecodesign and Analysis, pp. 445–464.
[29] Aabid, A., Hrairi, M., Abuzaid, A., Mohamed Ali, J.S. (2021). Estimation of stress intensity factor reduction for a center-cracked plate integrated with piezoelectric actuator and composite patch, Thin-Walled Struct., 158, DOI: 10.1016/j.tws.2020.107030.
[30] Achour, T., Bouiadjra, B.B., Serier, B. (2003). Numerical analysis of the performances of the bonded composite patch for reducing stress concentration and repairing cracks at notch, Comput. Mater. Sci., 28, pp. 41–48, DOI: 10.1016/S0927-0256(03)00054-5.
[31] Ouinas, D., Hebbar, A., Olay, J.V. (2006). Fracture Mechanics Modelling of Cracked Aluminium Panel Repaired with Bonded Composite Circular Patch, J. Appl. Sci., 6(9), pp. 2088–2095.
[32] Hosseini-Toudeshky, H., Mohammadi, B., Sadeghi, G., Daghyani, H.R. (2007). Numerical and experimental fatigue crack growth analysis in mode-I for repaired aluminum panels using composite material, Compos. Part A Appl. Sci. Manuf., 38, pp. 1141–1148, DOI: 10.1016/j.compositesa.2006.06.003.
[33] Oudad, W., Bouiadjra, B.B., Belhouari, M., Touzain, S., Feaugas, X. (2009). Analysis of the plastic zone size ahead of repaired cracks with bonded composite patch of metallic aircraft structures, Comput. Mater. Sci., 46(4), pp. 950–954, DOI: 10.1016/j.commatsci.2009.04.041.
[34] Barsoum, R.S. (1977). Triangular Quarter Point Elements as Elastic and Perfectly Plastic Crack Tip Elements, Int. j. Numer. Meth. Engng., 11(December 1975), pp. 85.
[35] Lei, Y., O'Dowd, N.P., Webster, G.A. (2000). Fracture mechanics analysis of a crack in a residual stress field, Int. J. Fract., 106(3), pp. 195–216, DOI: 10.1023/A:1026574400858.
[36] El-Emam, H.M., Salim, H.A., Sallam, H.E.M. (2017). Composite Patch Configuration and Prestress Effect on SIFs for Inclined Cracks in Steel Plates, J. Struct. Eng. (United States), 143(5), pp. 1–12, DOI: 10.1061/(ASCE)ST.1943-541X.0001727.
[37] Bouiadjra, B.B., Belhouari, M., Serier, B. (2002). Computation of the stress intensity factors for repaired cracks with bonded composite patch in mode I and mixed mode, Compos. Struct., 56, pp. 401–406.
[38] Bouiadjra, B.B., Belhouari, M., Ranganathan, N. (2000).Evaluation of the stress intensity factors for patched cracks with bonded composite repairs in mode I and mixed mode., pp. 1–8.